Taylor & Francis
Taylor & Francis Group

Biotechnology & Biotechnological Equipment

ISSN: 1310-2818 (Print) 1314-3530 (Online) Journal homepage: https://www.tandfonline.com/loi/tbeq20

Green synthesis of silver nanoparticles using aqueous leaf extract of *Premna integrifolia* (L.) rich in polyphenols and evaluation of their antioxidant, antibacterial and cytotoxic activity

Chandrashekhar Singh, Jitendra Kumar, Pradeep Kumar, Brijesh Singh Chauhan, Kavindra Nath Tiwari, Sunil Kumar Mishra, S. Srikrishna, Rajesh Saini, Gopal Nath & Jasmeet Singh

To cite this article: Chandrashekhar Singh, Jitendra Kumar, Pradeep Kumar, Brijesh Singh Chauhan, Kavindra Nath Tiwari, Sunil Kumar Mishra, S. Srikrishna, Rajesh Saini, Gopal Nath & Jasmeet Singh (2019) Green synthesis of silver nanoparticles using aqueous leaf extract of *Premna integrifolia* (L.) rich in polyphenols and evaluation of their antioxidant, antibacterial and cytotoxic activity, Biotechnology & Biotechnological Equipment, 33:1, 359-371, DOI: 10.1080/13102818.2019.1577699

To link to this article: https://doi.org/10.1080/13102818.2019.1577699

Published online: 12 Feb 2019.

BIOTECHNOLOGY & BIOTECHNOLOGICAL EQUIPMENT
2019, VOL. 33, NO. 1, 359–371
https://doi.org/10.1080/13102818.2019.1577699

Green synthesis of silver nanoparticles using aqueous leaf extract of *Premna integrifolia* (L.) rich in polyphenols and evaluation of their antioxidant, antibacterial and cytotoxic activity

Chandrashekhar Singh[a], Jitendra Kumar[b], Pradeep Kumar[a], Brijesh Singh Chauhan[c], Kavindra Nath Tiwari[a], Sunil Kumar Mishra[b], S. Srikrishna[c], Rajesh Saini[a], Gopal Nath[d] and Jasmeet Singh[e]

[a]Department of Botany, MMV, Banaras Hindu University, Varanasi, Uttar Pradesh, India; [b]Department of Pharmaceutical Engineering and Technology, Indian Institute of Technology, Banaras Hindu University, Varanasi, Uttar Pradesh, India; [c]Department of Biochemistry, Institute of Science, Banaras Hindu University, Varanasi, Uttar Pradesh, India; [d]Department of Microbiology, Institute of Medical Sciences, Banaras Hindu University, Varanasi, Uttar Pradesh, India; [e]Faculty of Ayurveda, Department of Dravyagun, Institute of Medical Sciences, Banaras Hindu University, Varanasi, Uttar Pradesh, India

ABSTRACT

Premna integrifolia L. is widely distributed in tropical and subtropical regions. In the present study, green silver nanoparticles were synthesized efficiently after mixing 1 mmol/L $AgNO_3$ and 4% aqueous leaf extract at neutral pH (7.0) after 25 min sunlight exposure. The aqueous leaf extract was enriched with polyphenols. It had higher flavonoid (67.23 ± 1.23 µg/mg gallic acid equivalent) than phenolic content (58.10 ± 2.29 µg/mg rutin equivalent). The bio-synthesized silver nanoparticles were characterized by different spectroscopic and microscopic studies. The synthesized nanoparticles were spherical in shape and ranged from 9 to 35 nm in size. The crystalline nature of the nanoparticles was confirmed on the basis of high-resolution transmission electron microscopy (HRTEM), high-resolution scanning electron microscopy (HRSEM), X-ray diffractometry (XRD) and selected area electron diffraction (SAED) analyses. The presence of silver ions in the biosynthesized nanoparticles was demonstrated based on energy-dispersive X-ray (EDX) data (3.5 keV). The functional groups involved in the nanoparticle synthesis were analysed using FT-IR. These silver nanoparticles showed good antibacterial activity against human pathogenic gram-positive (*Staphylococcus aureus*, *Enterococcus faecalis*) and gram-negative (*Shigella dysenteriae*, *Shigella flexneri* and *Vibrio parahaemolyticus*) bacteria. The silver nanoparticles exhibited good in vitro antioxidant and cytotoxic activity to human cervical cancer cell line (SiHa).

ARTICLE HISTORY
Received 9 October 2018
Accepted 30 January 2019

KEYWORDS
Premna integrifolia; silver nanoparticles; antimicrobial; cytotoxicity; antioxidants

Introduction

Nanotechnology is a rapidly growing area of scientific interest due to its wide applications in catalysis, solar energy, waste management and sensing technology. Nanomaterials are efficiently used in the field of medicine for the purpose of drug delivery, diagnosis, treatment of cardiovascular diseases, wound healing and development of antimicrobial agents. Recently, nanomaterials have expanded their application in cell labelling, biological tagging, cancer therapy, tissue engineering, DNA and protein detection [1]. Nanoparticles are synthesized by using different noble metals. They exhibit new physico-chemical properties which are not observed in either individual molecules or bulk metals [2]. Silver is a common metal used for synthesis of nanoparticles, which was accepted for its multipurpose applications. Nanoparticles synthesized via physical and chemical methods are highly expensive and toxic to the environment. Hence, there is a need for alternative methods of biosynthesis of nanoparticles. This biosynthesis should be cost-effective, rapid, easy, eco-friendly and nontoxic. Silver nanoparticles (AgNPs) prepared using biological materials, particularly plant materials [3], are small in size and have high surface area. Green synthesis of AgNPs is a one-step method and produces stable products [4]. Plant materials contain various phytoconstituents which reduce the silver ions into silver nanoparticles [5]. The formation, morphology and topography of plant-based nanoparticles is regulated by factors such as

CONTACT Kavindra Nath Tiwari kntiwaribhu@gmail.com Department of Botany, MMV, Banaras Hindu University, Varanasi, Uttar Pradesh, 221005, India

temperature, reaction incubation period [6], pH, plant extract concentration and $AgNO_3$ concentration [7]. Quick synthesis of green silver nanoparticles can be achieved under sunlight exposure without any use of instruments [8]. In previous reports, plant extracts of *Xanthium strumarium* and *Erigeron bonariensis* [8] were used for the synthesis of silver nanoparticles under sunlight exposure. Silver nanoparticles synthesized by using medicinal plant extracts have been utilized for various pharmaceutical applications [9] .

Premna integrifolia L. (Family Lamiaceae) is distributed in the tropical and subtropical regions of Asia, Africa and Australia [10]. In traditional medicine, it is used for the treatment of several health conditions. Extracts of root, bark and wood show wide antimicrobial activities [11]. This plant possesses an excellent antioxidant activity [12]. Cytotoxic effects of leaf methanolic extract on liver (HepG2), breast (MCF7) and lung (A549) cancer cell lines have previously been reported [13]. The growth of ehrlich ascites carcinoma (EAC) cell lines [14] was arrested by ethanolic extract of leaf.

The present study aimed to synthesize silver nanoparticles by using aqueous leaf extract of *P. integrifolia*. Characterization of these nanoparticles was based on spectroscopy and microscopy. We evaluated the *in vitro* antioxidant activity of the synthesized nanoparticles as well as their antibacterial activity against gram-positive (*Staphylococcus aureus* and *Enterococcus faecalis*) and gram-negative (*Shigella dysenteriae, Shigella flexneri* and *Vibrio parahaemolyticus*) pathogenic bacteria. The cytotoxicic potential of the synthesized nanoparticles was examined against a human cervical cancer cell line (SiHa) by using MTT assay.

Materials and methods

Collection of plant material and preparation of the extract

About 25 g of fresh *P. integrifolia* leaves were collected from the Ayurvedic Garden of Banaras Hindu University, Varanasi, UP, India. The leaves were washed thoroughly under running tap water, cut into small pieces and heated for half an hour in 100 mL deionized water at 50°C. The aqueous leaf extract of *P. integrifolia* (AEP) was cooled and filtered through Whatman filter paper No.1 (pore size 25 μm) and stored at 4°C for further applications.

Measurement of total phenolic content (TPC)

The TPC in the aqueous leaf extract was determined by Folin–Ciocalteu method as previously reported by McDonald et al. [15] with some modifications. Briefly, 1 mL distilled water, 0.1 mL of 1 mg/mL AEP and 0.2 mL of Folin–Ciocalteu reagent were added in a test-tube and mixed thoroughly and allowed to stay for 5–8 min at room temperature. Furthermore, the solution was neutralized with 2 mL of 7% sodium carbonate solution, followed by maintaining the volume of the reaction mixture up to 3 mL by adding 0.7 mL distilled water. Subsequently, solutions were mixed and allowed to stand at room temperature for 15 min, and then absorbance was noted at 750 nm. Phenol content was estimated by using a standard curve obtained from various concentrations of gallic acid. The results were expressed as micrograms per miligram of gallic acid equivalents (GAE).

Measurement of total flavonoid content (TFC)

Determination of TFC in the extract was done by $AlCl_3$ colourimetric method [16]. Aliquots of AEP (0.1 mL of 10 mg/mL) in ethanol were mixed with an equal volume of 2% $AlCl_3$, 0.1 mL of 1 mol/L potassium acetate and 2.7 mL of ethanol. The reaction mixture was vigorously shaken, kept at room temperature for 30 min and absorbance was recorded at 415 nm. TFC was calculated using rutin as the standard and was expressed as micrograms per miligram of rutin equivalents (RE).

Biosynthesis of silver nano particles (AEP-AgNPs)

For the synthesis of nanoparticles, 4% AEP was added to 1 mmol/L aqueous silver nitrate ($AgNO_3$; 100 mL) solution in a conical flask. The pH of the reaction mixture was adjusted to 7 (neutral). The flask containing the reaction mixture was kept under bright sun light (65000 lux) at 38 ^{0}C. To optimize the biosynthesis of AEP-AgNPs, different factors such as sunlight exposure duration (0–30 min), $AgNO_3$ concentration (0.5–5 mmol/L) and AEP inoculum dose (0.5–6.0%) were evaluated one at a time under bright sunlight. AEP-AgNPs synthesized at the optimum conditions were purified by centrifugation at 15,000 rpm for 30 min (CM 12 plus, REMI, India) and re-dispersed in de-ionized water to eliminate the water-soluble biological residues. The process was repeated four times, and the pellet/sediment was dried at room temperature for final mass of AEP-AgNPs to be used in further studies.

Characterization

Several techniques were employed to characterize the silver nanoparticles. Confirmation of the biosynthesis

of AEP-AgNPs was based on the colour change in the reaction mixture. The optical density of the reaction mixture was recorded with a UV–Visible spectrophotometer (Simadzu1800) by scanning the spectra in the range of 200–800 nm. The morphology of the nanoparticles was studied with the help of high-resolution scanning electron microscopy (HRSEM; Nova Nano SEM450) at 10 kV (accelerating voltage). For this analysis, 1 nA was maintained up to 7 s. Energy-dispersive X-ray (EDX) equipped with HRSEM was useful for the analysis of elemental composition and purity of the sample. For HRSEM-EDX analysis, a drop of ultrasonicated colloidal re-dispersed mass of AEP-AgNPs was dried over thin aluminum foil (under table lamp) for 2 h and coated with gold. AEP-AgNPs size and morphology were studied by high-resolution transmission electron microscopy (HRTEM; TECHNI G2 20 TWIN; FEI). This was conducted at 200 kV accelerating voltage. For HRTEM analysis, a drop of AEP-AgNPs was placed on a carbon coated copper grid, dried at room temperature for 2 h and loaded onto the specimen holder. The average particle size during HRTEM analysis was calculated by using 'Image J' software. The XRD pattern of AEP-AgNPs was determined by an X-ray diffractometer (Rigaku Miniflex 600), which was equipped with a Cu Kα radiation source and Ni filter in the range of 20–80° at a scanning rate of 2°/min. To determine the average particle size of the AgNPs, we applied the Debye–Scherrer equation:

$$D = K\lambda/\beta\cos\theta,$$

where D is the average crystallite domain size, perpendicular to the reflecting planes; K is Scherer's constant, its value ranging between 0.9 and 1; λ represents the wave length of the X-ray source (0.1541 nm) used in XRD; β denotes the full width at the half maximum of the diffraction peak and θ is the diffraction angle. Selected area electron diffraction (SAED) was studied to confirm the crystalline nature of the nanoparticles. The functional groups involved in the reduction of the Ag^{+} ions and capping of the phytofabricated AEP-AgNPs were studied using of Fourier transform infrared spectroscopy (FT-IR; Bruker Germany) in the range of 4000–400 cm^{-1}. Atomic force microscopy (AFM) was used to analyse the surface texture of AEP-AgNPs (NT-MDT, Russia) in the contact mode. The images were processed using NOVA software. For its analysis of AFM, a single drop of colloidal AEP-AgNPs was spin-coated over a small slide and dried under a table lamp for 2.30 h.

Evaluation of antioxidant activity via DPPH assay

DPPH radical scavenging assay for AEP and AEP-AgNPs was carried out as described by Chang et al. [16]. Ascorbic acid was used as the reference. DPPH solution (0.004%) was prepared by dissolving in methanol. DPPH solution (2.96 mL) was added to different concentration of samples (50–700 μg/mL) prepared in methanol. This reaction mixture was kept at room temperature in darkness for 20 min. The absorbance of the reaction mixture was recorded after 20 min with a UV–Vis spectrophotometer at 517 nm. DPPH was used as the control. The following equation was used for the calculation of percentage inhibition: $[(\text{Absorbance}_{\text{control}} - \text{Absorbance}_{\text{sample}})/(\text{Absorbance}_{\text{control}})] \times 100$. The mean and standard deviation (SD) were calculated by repeating all the experiments three times.

Antimicrobial activity of AEP-AgNPs

Microorganisms and inoculum preparation

The antibacterial activities of AEP and AEP-AgNPs were evaluated against both gram-positive (*S. aureus* and *E. faecalis*) and gram-negative (*S. dysenteriae, S. flexneri*, and *V. parahaemolyticus*) clinical bacterial isolates. The clinical isolates were obtained from the Department of Microbiology, Institute of Medical Sciences, Banaras Hindu University, Varanasi, UP, India. Bacterial cultures for antimicrobial assay were maintained on nutrient agar (NA) slants by picking a colony from 24-h old Mueller-Hinton agar (MHA) plates. For standardized populations, a single bacterial colony was selected and transferred using a sterile loop into Mueller-Hinton broth (MHB) and continuously shaken at 100 rpm at 37°C overnight. For the antibacterial activity assay, the optical densities of bacterial suspensions were maintained equal to 0.5 MacFarland standards by adding sterile MHB broth. Thus, the resultant inoculum would comprise a bacterial number of approximately 10^6–10^7 CFU/mL.

Determination of minimal inhibitory concentration (MIC)

To determinate the MIC values, the agar dilution susceptibility test was adopted from a standard microbiological method [17]. In the agar dilution method, two-fold serial dilutions of AEP and AEP-AgNPs were prepared in 25 mL complete molten MHA medium, cooled down at 45°C and poured into Petri dishes (100 cm^2), which resulted an agar thickness of 2.5 mm. The desired final concentrations in the agar

plates ranged from 99.0 to 0.16 μg/ml for AEP-AgNPs and 165.0 to 0.65 μg/mL for AEP. Bacterial suspensions (5 μL) were inoculated on solid MHA plates. These agar plates were further incubated at 37°C for 48 h. The MIC values were calculated as the lowest concentration of synthesized AEP-AgNPs and AEP that completely inhibits bacterial growth on solid medium.

Cytotoxicity study

To test the cytotoxicity activity of AEP and its nano formulation (AEP-AgNPs) in SiHa cells, MTT [3-(4, 5-dimethylthiazolyl-2)-2, 5-diphenyltetrazolium bromide] assay was performed. For this, 1×10^3 SiHa cells were seeded in Dulbecco's Modified Eagle's Medium (DMEM) with 10% Fetal bovine serum (FBS) in 96 well cell culture plate (Genetix Biotech Asia Pvt. Ltd). To test the viability of cells, initially cells were exposed with various concentrations (10, 50, 100, 250 and 500 μg/mL) of plant extract and nanomaterials, incubated for 24 h at 37 °C in CO_2 incubator (Binder model C150) in dark condition. The cells treated with DMEM medium alone were considered as a control. After incubation, plant extract and formulation were removed and cells were incubated with 100 μL of 0.5 mg/ml MTT each for another 2 h at 37 °C in darkness in a CO_2 incubator. After the incubation, cells were washed twice with 1X phosphate buffered saline (PBS; pH 7.4) and treated with 100 μL of DMSO (dimethyl sulfoxide) for an additional 1 h at 37 °C to dissolve the purple coloured formazan crystals. The purple coloured solutions of each sample were transferred into discrete wells of cell culture plates. The absorbance strength of the colour solutions was measured at 575 nm by a Multimode plate reader (Synergy H1 Biotek). All the experiments were carried out in triplicate and cell viability was expressed in percentage in relation to the control.

Results and discussion

Total polyphenol content

In the obtained AEP, the total phenol content (TPC) and the TFC were 58.10 ± 2.29 μg/mg GAE and 67.23 ± 1.23 μg/mg RE, respectively (Figure 1). Medicinal plant extracts contains different constituents with several functional groups, which act as reducing agents for Ag^+ ions to silver nanoparticles. Extracts of leaves [18], stems [19], fruit [20], bark [21] and root [22] have potential for reduction of Ag^+ ions to silver nanoparticles as reported by several works.

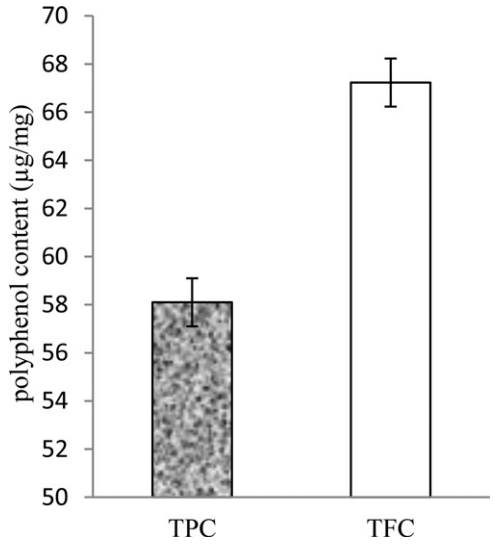

Figure 1. Total phenol and flavonoid content in aqueous leaf extract of *P. integrifolia*. Note: Values are means ± SD ($N = 3$).

Visual confirmation of synthesis of silver nanoparticles by UV–Vis spectroscopy

Leaf extract (green) of *P. integrifolia* was added in $AgNO_3$ solution (colourless) and it was kept for 25 min under bright sunlight. The colour of the solution changed from dark green to dark orange (Figure 2(a)), reflecting the biosynthesis of AEP-AgNPs. UV–Vis spectral analysis showed a surface plasmon resonance peak at 417 nm, which confirmed the AEP-AgNPs biosynthesis (Figure 2(b)). In a previous report, a surface plasmon resonance (SPR) peak ranging 400–500 nm suggested AgNP formation [23]. Several factors like the shape and size of nanoparticles present in the reaction mixture as well as the type of surrounding media affect the SPR absorbance.

Optimization of factors for biosynthesis of AEP-AgNPs

Reaction mixtures containing 1 mL of 4% (v/v) AEP solution and 10 mL of 1 mmol/L silver nitrate were exposed to bright sunlight for different time intervals (0 to 30 min). There was a time-dependent continuous increase in the optical density. After 25 min sunlight exposure, the maximum SPR band at 417 nm was recorded. However, after 30 min sunlight exposure, there was no further change in the absorbance, indicating that there was no further effect on the SPR band (Figure 2(c)).

To optimize the inoculum concentration (AEP) for good nanoparticle synthesis, reaction mixtures containing different concentrations (0.5–6%) of AEP and 1 mmol/L $AgNO_3$ were exposed to bright sunlight for 25

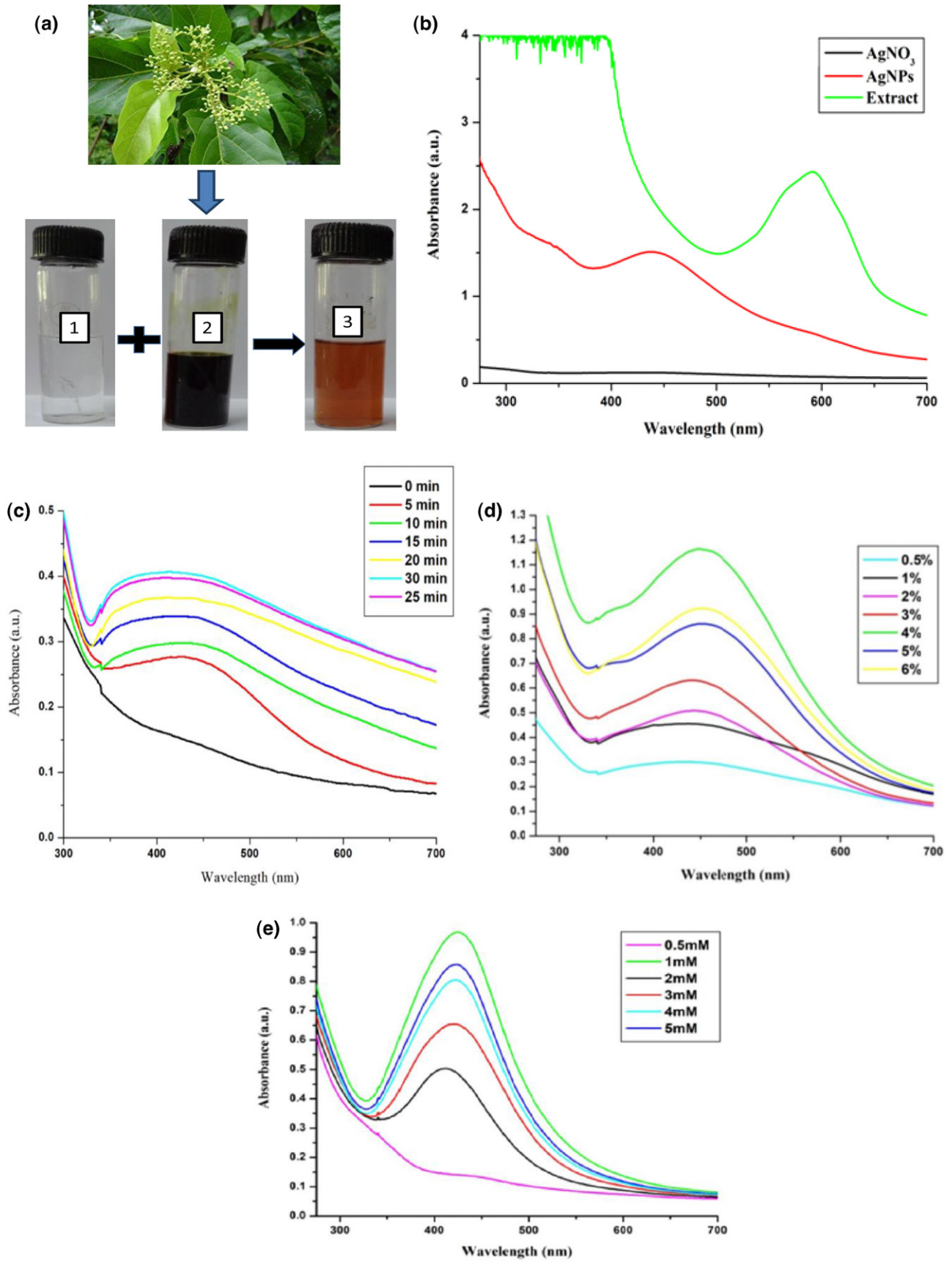

Figure 2. Biosynthesis of silver nanoparticles (a): *P. integrifolia* plant, aqueous silver nitrate solution (1), aqueous leaf extract (2), silver nanoparticles (AEP-AgNPs) (3); (b): UV-Vis spectra; (c): UV–Vis absorbance spectra peak of prepared AEP-AgNPs at different time intervals during sunlight exposure; (d): UV–Vis spectra of AEP-AgNPs prepared at different inoculum doses (%) of AEP; (e): UV–Vis spectra of AEP-AgNPs prepared at different silver nitrate concentrations (mmol/L).

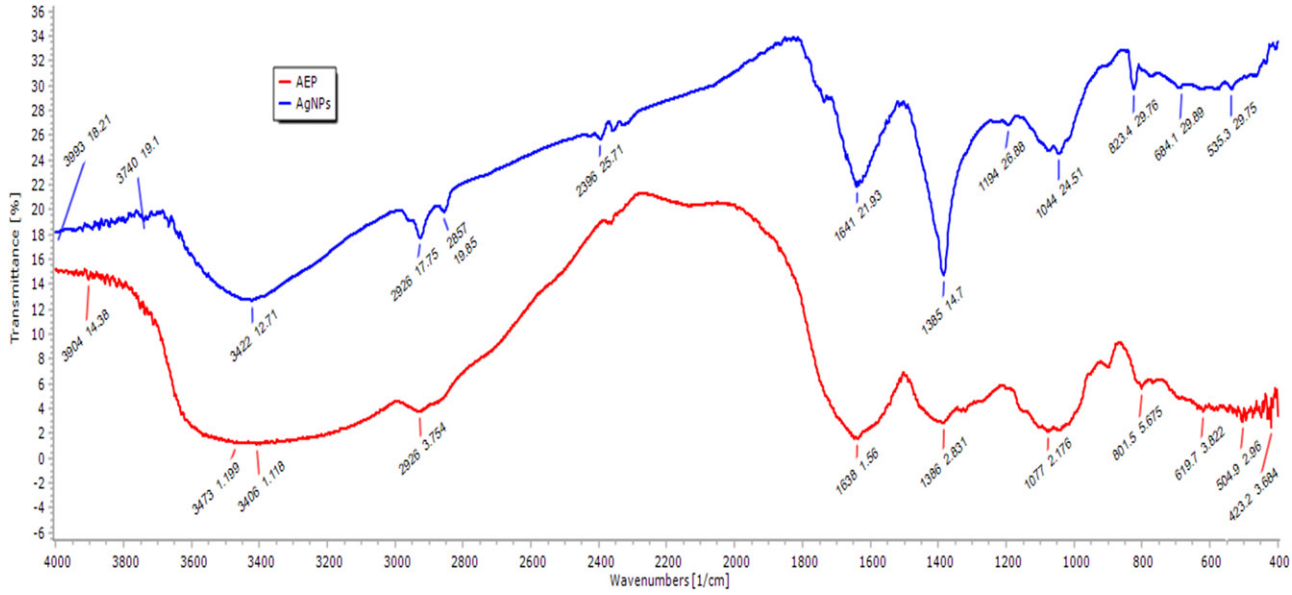

Figure 3. FT-IR spectra of aqueous leaf extract of *P. integrifolia* (AEP) and AEP-AgNPs.

min (Figure 2(d)). The absorption increased with the increase in AEP concentration. The results revealed that the absorbance was maximum at 4% AEP. Beyond 4% AEP concentration (5–6%), there was no considerable change in the absorption maxima.

Reaction mixture containing 4% AEP solution along with varying concentrations of silver nitrate (0.5–5 mmol/L) exposed to sunlight for 25 min revealed AEP-AgNPs biosynthesis, which was confirmed by UV–Vis spectral analysis (Figure 2(e)). At 1 mmol/L $AgNO_3$, the absorption of the reaction mixture reached a maximum. The test solutions containing 2–5 mmol/L $AgNO_3$ exhibited a lower absorption in comparison to 1 mmol/L $AgNO_3$.

The FT-IR spectra of AEP showed peaks at 3422, 2926, 2857, 2396, 1641, 1385, 1194, 1044 and 823 cm^{-1}. In AEP-AgNPs, the FT-IR spectrum peaks at 2857 and 1194 cm^{-1} were missing. The peak at 3422 cm^{-1} represents the H-bonded O–H stretch. The peak at 2926 cm^{-1} corresponds to side chain vibrations consisting of C–H stretching and indicating the presence of $–NH_2$ groups. The peak at 2857 cm^{-1} suggests methylene C–H stretching. Peak 2396 cm^{-1} corresponds to the absorption of a triple bond [24]. The peak at 1641 cm^{-1} corresponds to N–H bending vibrations, while the one at 1385 cm^{-1} represents aromatic nitro compounds. Peaks 1194, 1044 and 823 cm^{-1} correspond to C–H bending vibrations in aromatic rings. The FT-IR results revealed that the bioreduction of silver ions during the biosynthesis of AEP-AgNPs was due to reduction by capping material in the plant extract with the functional groups of these regions (2857 and 1194 cm^{-1}) (Figure 3) . FT-IR spectroscopy is important in probing the functional groups of compounds. It is frequently used in characterizing plant extracts and nanoparticles synthesized from such extracts. The two important events, reduction and capping, contribute significantly during the process of AgNPs synthesis. In these processes, different functional groups present in different phytoconstituents of the extracts, such as alkaloids, amino acids, flavonoids, saponins, steroids, glycosides, carbohydrates, tannins and phenolics, are involved in the formation and stabilization of nanoparticles by forming different linkages with silver ions. The extract rich in polyphenols contributed a major role in the synthesis of stable nanoparticles. Changes in the intensity and small shifts were observed in the spectra of the extract and the nanoparticles. This may be due to co-ordination of phytochemicals with metal surface [25]. Important linkages such as C = O, –C–OC–, N–H, –C = C–, –C = C–H and C–H are formed during the process of nanoparticle synthesis [24]. Similar linkages were also observed in the present investigation.

The crystalline nature of dried AEP-AgNPs was studied through XRD analysis. The XRD pattern of AEP-AgNPs is shown in Figure 4. There were four distinct diffraction peaks at 38.2, 44.4, 64.5, and 77.5, respectively corresponding to (111), (203), (220) and (311) planes of face-centered cubic crystal structure of metallic silver (JCPDS file no.040783).

According to the Debye–Scherrer equation, the average particle size was calculated to be 20 nm. The diffraction peaks recorded during XRD as well as the bright circular ring pattern observed in SAED suggested that the AEP-AgNPs had crystalline nature.

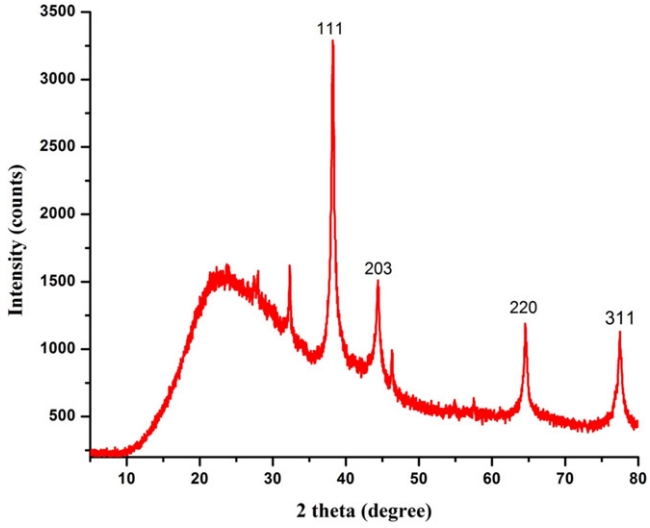

Figure 4. X-ray diffraction pattern of synthesized AEP-AgNPs using aqueous leaf extract of *P. integrifolia*.

Similar XRD and SAED patterns were recorded in *Erigeron bonariensis* [26]. EDX analysis of SEM revealed the presence of elemental silver in the synthesized AEP-AgNPs.

The HRTEM images of the AEP-AgNPs (Figure 5(a,b)) showed that the synthesized nanoparticles were highly stabilized and were spherical in shape with smooth surface. The crystalline nature of the silver nanoparticles was also confirmed from SAED pattern analysis (Figure 5(c)). The particle size distribution of the AEP-AgNPs was between 5 and 15 nm, with an average particle size of 9 nm (Figure 5(d)). The HRSEM analysis data showed that the synthesized AEP-AgNPs were spherical in shape of various sizes ranging between 9 and 35 nm (Figure 6(a)). Some nanoparticles were bigger in size, which may be due to aggregation or overlapping of particles. The size, shape and morphology of the synthesized green nanoparticles were confirmed by HRTEM and HRSEM imaging. These techniques have been frequently used by different workers [23,27] for characterization of nanoparticles. TEM and SEM images of the AEP-AgNPs confirmed that these nanoparticles were highly stabilized and were spherical in shape with smooth surface. Biosynthesis of smooth and spherical nanoparticles has been reported in *Sida cordifolia* [28]. These images indicate the formation of aggregates of nanoparticles. In these aggregates, the particles were not directly attached to each other. This suggests that the nanoparticles were stabilized by the aqueous extract of *P. integrifolia*, which acted as a capping agent.

The EDX spectra of silver nanoparticles were recorded between 2–4 keV, which clearly showed a strong spectral signal in the silver region at 3.5 keV (Figure 6b). The SPR of AgNPs strongly supports the formation of AEP-AgNPs. In the EDX spectra, the presence of signals of oxygen, nitrogen and carbon suggests the presence of biomolecules (carbohydrates and proteins) adjacent to AEP-AgNPs.

AFM is an ideal characterization tool for surface texture and particle size distributions of biosynthesized nanoparticles. Based on AFM, we took 2 D (Figure 7a) and 3 D (Figure 7b) pictures of the AEP-AgNPs. Based on these pictures, the average surface roughness of the AEP-AgNPs was calculated (9.69 nm). The AFM data revealed the maximum profile peak height and valley depth, which were 32.0 and 31.65 nm, respectively (Figure 7(c)).

Antioxidant activities

The antioxidant activity of AEP and AEP-AgNPs was assessed by DPPH scavenging assay using ascorbic acid as a positive control. The free-radical scavenging activity of AEP and AEP-AgNPs was directly related with their concentration. The EC_{50} values of AEP and AEP-AgNPs were 715.23 ± 1.26 and 524.19 ± 2.63 μg/mL, respectively. These results revealed that the AEP-AgNPs had greater free-radical scavenging potential than AEP (Figure 8(a)). The reducing power of compounds is directly proportional to their antioxidant activity. DPPH is a stable compound and accepts hydrogen or electrons from silver nanoparticles. This assay is frequently used in the measurement of free-radical scavenging capacity of compounds present in medicinal plant extracts [29]. This assay revealed the free-radical scavenging nature of AEP and AEP-AgNPs. The scavenging potential of AEP and AEP-AgNPs increased in a concentration-dependent manner. The scavenging activity of AEP-AgNPs was many times

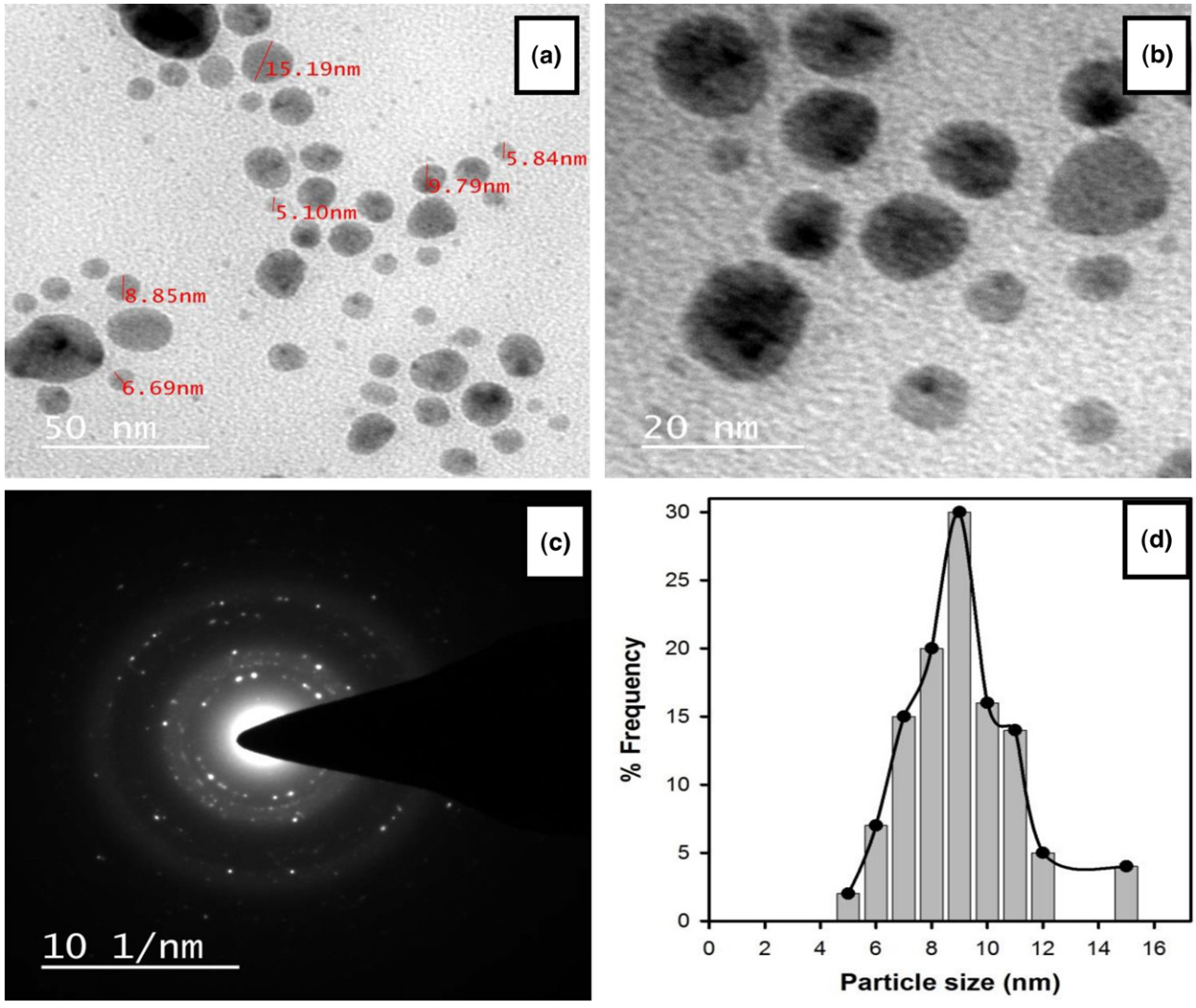

Figure 5. HRTEM images of AEP-AgNPs at different magnifications (a and b), SAED pattern of AEP-AgNPs (c) and size distribution histogram (d).

greater than that of AEP. Similar observations of enhanced DPPH scavenging activity by gold, platinum, selenium and silver nanoparticles have already been reported by various workers [30,31].

Evaluation of antimicrobial activities

We explored the antimicrobial activity of AEP and AEP-AgNPs against two gram-positive (*S. aureus* and *E. faecalis*) and three gram-negative (*S. dysenteriae*, *S. flexneri* and *V. parahaemolyticus*) clinical isolates *in vitro* (Figure 8(b)). The MIC value of the synthesized AEP-AgNPs (16.5–66 μg/mL) was lower than that of AEP (82–145 μg/mL). The tested gram-negative bacterial isolates were more susceptible (AEP MIC: 82.17–104.0 μg/mL; AgNPs MIC: 16.5–59.28 μg/mL) than the gram-positive ones (AEP MIC: 121.19–145.17 μg/mL; AEP-AgNPs MIC: 33.2–66.42 μg/mL) for AEP and AEP-AgNPs. If we compare the susceptibility among the tested bacteria, *V. parahaemolyticus* was most susceptible and *E. faecalis* was least susceptible to AEP and AEP-AgNPs.

Medicinal plants, due to their antimicrobial activity, are used in traditional medicine for the treatment of a range of diseases [32]. The AEP and AEP-AgNPs exhibited good antibacterial activity against both gram-negative and gram-positive clinical isolates. Our observation that the MIC value of AEP was greater than that of AEP-AgNPs suggests that silver nanoparticles have stronger antibacterial activity than the extract alone. The superiority of phytosynthesized AgNPs as compared to the respective plant extracts in terms of strong antibacterial action has also been reported in earlier studies [33]. This superiority of nanoparticles may be based on their size and large surface area. The small size of nanoparticles helped in easy penetration

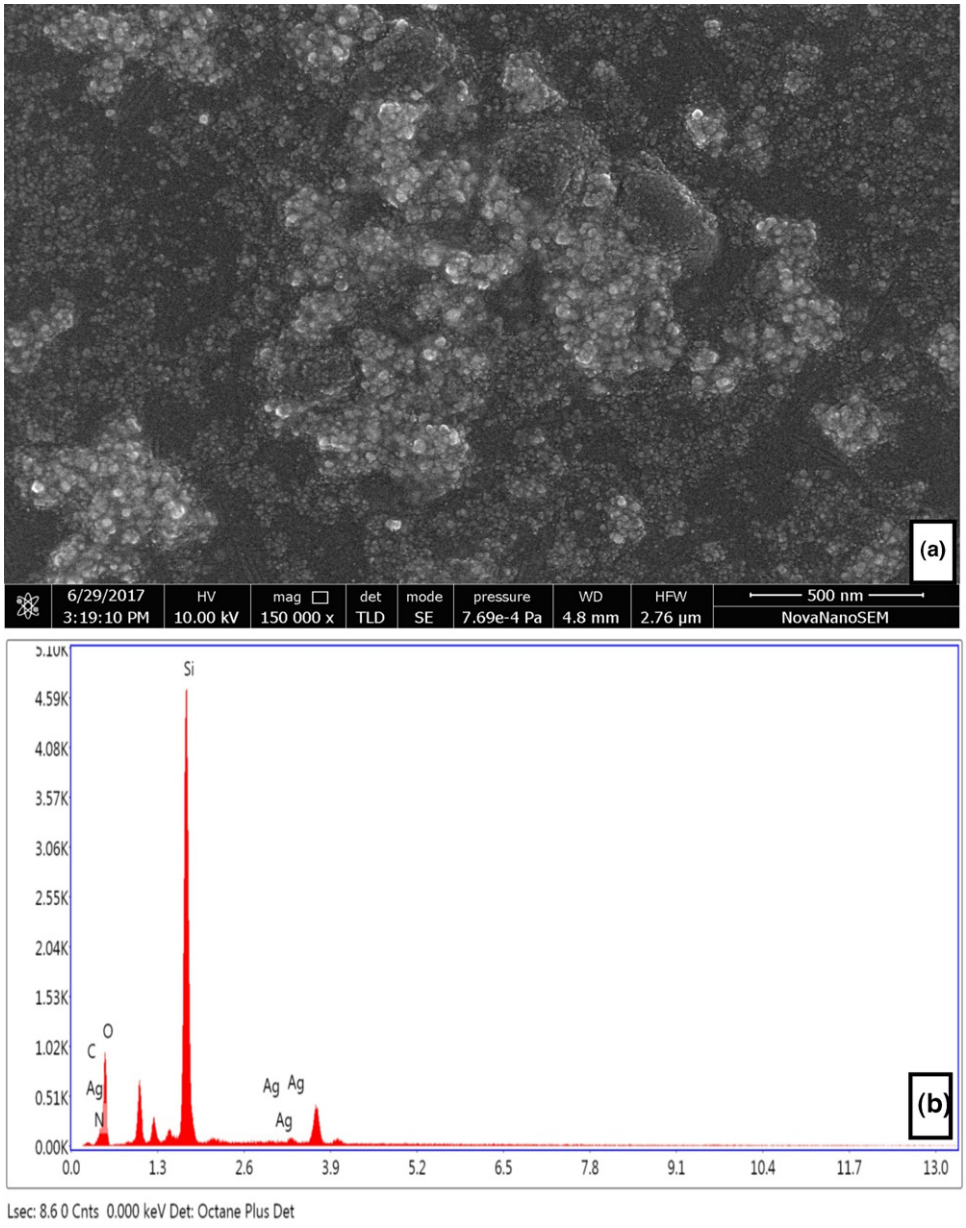

Figure 6. HRSEM micrograph of AgNPs synthesized using aqueous leaf extract of *P. integrifolia* (a) and energy dispersive X-ray spectrum of AEP-AgNPs (b).

and large surface area support for better contact with microbes, which facilitates strong antimicrobial action. In this study, we observed stronger antibacterial activity of AEP and AEP-AgNPs against gram-negative bacteria (*S. dysenteriae, S. flexneri* and *V. Parahaemolyticus*) than against gram-positive bacteria (*S. aureus* and *E. faecalis*). This differential activity may be due to differences in bacterial cell wall structure and composition. The cell wall of gram-positive bacteria is rich in peptidoglycan as compared to gram-negative bacteria [34]. Peptidoglycan is formed by the cross-linking of short peptides with linear polysaccharides, which contributes to its rigidness. It creates a barrier against the penetration of silver nanoparticles. Biologically synthesized AEP-AgNPs are promising therapeutic agents demonstrating significant antimicrobial and cytotoxic action. Biosynthesized nanoparticles have been described for their ability to inhibit/destroy microbial cells. Nanoparticles may be good source for delivery of herbal medicines in the field of health promotion [35].

Cytotoxicity of AEP and AEP-AgNPs against SiHa cells

Cervical cancer is the second most common malignancy reported among women worldwide. It shows high resistance against radiotherapy. In the present

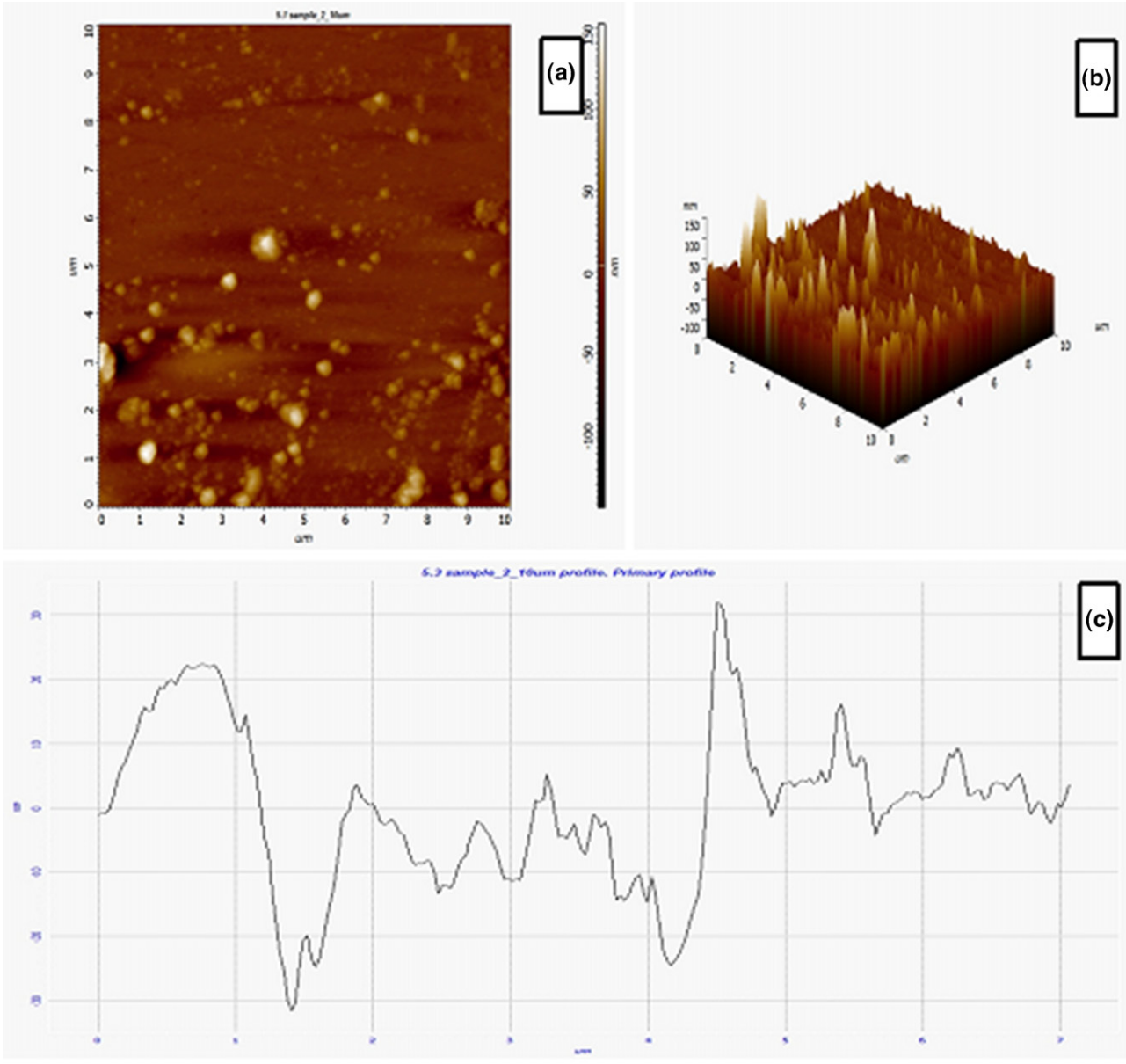

Figure 7. AFM images of green synthesized AgNPs using *P. integrifolia* aqueous leaf extract: 2D (a) and 3D view (b) and roughness profile (c) of AEP-AgNPs.

study, MTT assay was performed to determine the effect of AEP and AEP-AgNPs on the metabolic activity of SiHa cells *in vitro*. The untreated cells were considered as control cells, i.e. 100% cell viability (Figure 8(c)). The cells treated with AEP-AgNPs in concentrations of 10, 50 and 100 μg/mL demonstrated better cell viscosity, indicating that AEP-AgNPs were less cytotoxic than AEP. Higher concentrations of AEP-AgNPs (500 μg/mL) greatly reduced the viability of cells in contrast to AEP alone (Figure 8(c)). These results suggested that, at lower concentrations of nano-formulation, the cells were metabolically more active than at equivalent AEP concentrations, whereas at higher concentrations (500 μg/mL), the cancer cell metabolic activity was greatly reduced by the AEP-AgNPs. Hence, the final outcome indicates that the nanoformulation of AEP-AgNPs showed a higher cytotoxicity than AEP at 500 μg/mL in SiHa cells, clearly reflecting the increased potential of our biologically synthesized silver nanoparticles against this cancer cell line.

A few *in vitro* studies have analysed the movement of silver nanoparticles in cancer cell lines with IC_{50} value of 100 μg/mL [36]. AgNPs synthesized from *Piper longum* fruit extract exhibited cytotoxic effect (IC_{50}) at 67 μg/mL against the Hep-2 cell line [37]. Similarly, nanoparticles synthesized from *Origanum vulgare* exhibited LD_{50} of 100 μg/mL in the human lung

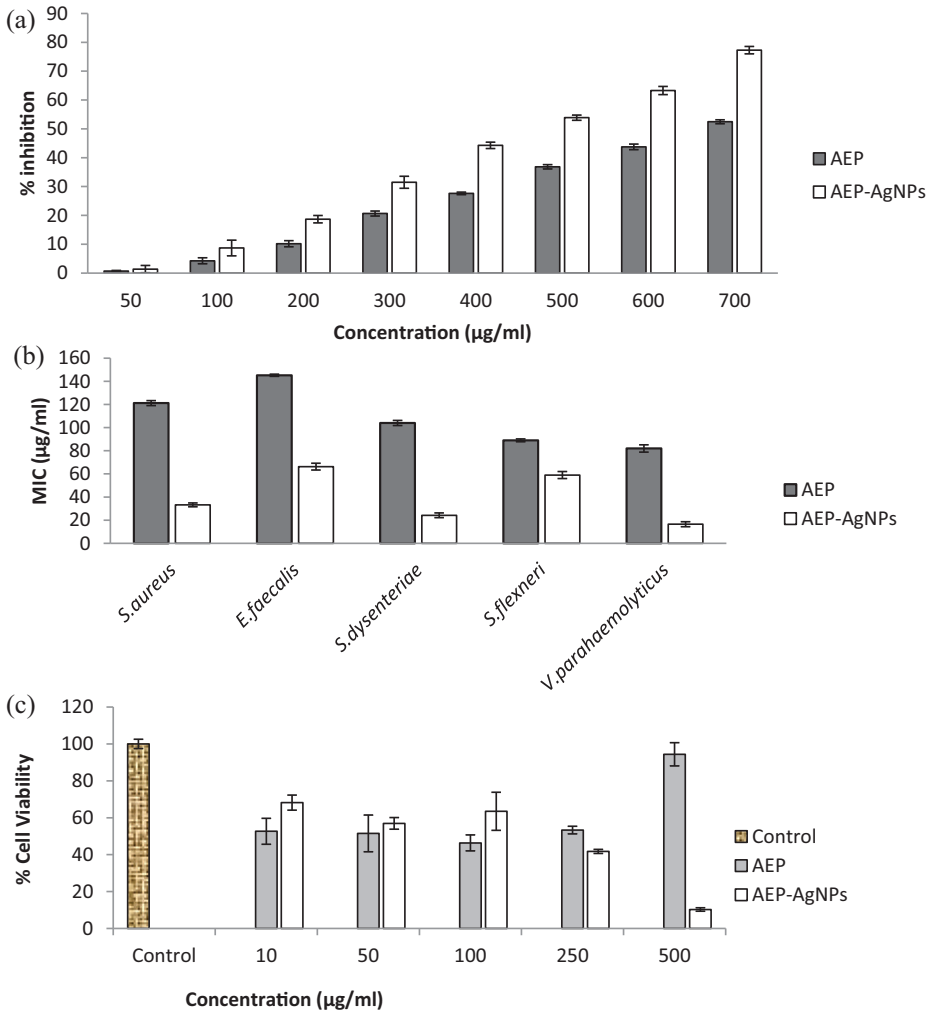

Figure 8. Antioxidant (a), antimicrobial (b) and cytotoxic (c) activity of aqueous leaf extract (AEP) and silver nanoparticles synthesized using aqueous leaf extract of *P. integrifolia*.

cancer cell line A549 [38]. In fact, silver nanoparticles may induce reactive oxygen species, which cause damage to cellular components such as DNA, proteins and lipids and ultimately lead to death of cancer cells [39]. To the best of our knowledge, the present study is the first report of cytotoxic effect of AEP-AgNPs against a human cervical cancer cell line. The improved cytotoxic effect of *P. integrifolia* AgNPs may be due to small size and quick entry inside the cells. Further investigation is required to identify the possible mechanisms involved in the cytotoxic activity.

Conclusions

Polyphenol rich aqueous leaf extract of medicinally important *P. integrifolia* was effectively used to synthesise stable AgNPs in the presence of sunlight. The biosynthesis of AEP-AgNPs was confirmed using UV–Vis, FT-IR, HRSEM, EDX, XRD, HRTEM and AFM. The AEP-AgNPs demonstrated significant antioxidant, antibacterial and cytotoxic activity against a cervical cancer cell line (SiHa). The improved cytotoxic effect of *P. integrifolia* may be attributed to the presence of bioactive compounds and fast entry inside the cells. Future investigations need to focus on identifying the possible mechanisms underlying the cytotoxicity activity.

Acknowledgements

Author C. Singh, P. Kumar and K.N. Tiwari would like to acknowledge University Grants Commission (UGC), Government of India, for financial assistance. The authors appreciate the Central Instrument Facility (CIF), Indian Institute of Technology (BHU), Varanasi, India for characterization of nanoparticles.

Disclosure statement

The authors hereby declare that there is no conflict of interest regarding this paper.

References

[1] Liu X, Bing T, Shangguan D. Microbead-based platform for multiplex detection of DNA and protein. ACS Appl Mater Interf. 2017;9:9462–9469.

[2] Dauthal P, Mukhopadhyay M. Noble metal nanoparticles: Plant-mediated synthesis, mechanistic aspects of synthesis, and applications. Ind Eng Chem Res.. 2016;55:9557–9577.

[3] Ahmed S, Ahmad M, Swami BL, et al. A review on plants extract mediated synthesis of silver nanoparticles for antimicrobial applications: a green expertise. J Adv Res. 2016;7:17–28.

[4] Mittal J, Batra A, Singh A, et al. Phytofabrication of nanoparticles through plant as nanofactories. Adv Nat Sci: Nanosci Nanotechnol.. 2014;5:043002. [cited 2018 Oct 31][10 p.]

[5] Caro C, Castillo PM, Klippstein R, et al. Silver nanoparticles: sensing and imaging applications. In: Pozo D, editor. Silver nanoparticles. London (UK): InTech; 2010.

[6] Sun Y, Xia Y. Shape-controlled synthesis of gold and silver nanoparticles. Science. 2002;298:2176–2179.

[7] Ibrahim HM. Green synthesis and characterization of silver nanoparticles using banana peel extract and their antimicrobial activity against representative microorganisms. J Radiat Res App Sci. 2015;8:265–275.

[8] Kumar V, Gundampati RK, Singh DK, et al. Photo-induced rapid biosynthesis of silver nanoparticle using aqueous extract of *Xanthium strumarium* and its antibacterial and antileishmanial activity. Ind. Eng. Chem. Res. 2016;37:224–236.

[9] Thota S, Crans DC. *Metal nanoparticles: synthesis and applications in pharmaceutical sciences*. Hoboken: Wiley; 2018.

[10] Munir AA. A taxonomic revision of the genus *Premna* L.(Verbenaceae) in Australia. *J Adel Bot Gard*. 1984;7: 1–43.

[11] Rahman A, Shanta ZS, Rashid M, et al. In vitro antibacterial properties of essential oil and organic extracts of *Premna integrifolia* Linn. Arab J Chem. 2016;9:S475–S479.

[12] Habtemariam S, Varghese GK. A Novel Diterpene Skeleton: Identification of a highly aromatic, cytotoxic and antioxidant 5-methyl-10-demethyl-abietane-type diterpene from *Premna serratifolia*. Phytother Res.. 2015;29:80–85.

[13] Selvam TN, Venkatakrishnan V, Damodar KS, et al. Antioxidant and tumor cell suppression potential of *Premna serratifolia* linn leaf. Toxicol Int.. 2012;19:31

[14] Sridharan G, Brindha P, Jaiganesh C, et al. Anti tumor potential of *Premna integrifolia* Linn. against Ehrlich ascites carcinoma cell lines. Pharmacologyonline. 2011;2:438–450.

[15] McDonald S, Prenzler PD, Antolovich M, et al. Phenolic content and antioxidant activity of olive extracts. Food Chem. 2001;73:73–84.

[16] Chang C-C, Yang M-H, Wen H-M, et al. Estimation of total flavonoid content in *Propolis* by two complementary colorimetric methods. J Food Drug Anal. 2002;10:178–182.

[17] Klančnik A, Piskernik S, Jeršek B, et al. Evaluation of diffusion and dilution methods to determine the antibacterial activity of plant extracts. J Microbiol Methods. 2010;81:121–126.

[18] Dehghanizade S, Arasteh J, Mirzaie A. Green synthesis of silver nanoparticles using *Anthemis atropatana* extract: characterization and in vitro biological activities. Artif Cells Nanomed Biotechnol. 2018;46: 160–168.

[19] Paulkumar K, Gnanajobitha G, Vanaja M, et al. *Piper nigrum* leaf and stem assisted green synthesis of silver nanoparticles and evaluation of its antibacterial activity against agricultural plant pathogens. Sci World J. 2014;2014:1–9.

[20] Ramesh P, Kokila T, Geetha D. Plant mediated green synthesis and antibacterial activity of silver nanoparticles using *Emblica officinalis* fruit extract. Spectrochim Acta A: Mol Biomol Spectrosc. 2015;142: 339–343.

[21] Arya G, Kumari RM, Gupta N, et al. Green synthesis of silver nanoparticles using *Prosopis juliflora* bark extract: reaction optimization, antimicrobial and catalytic activities. Artif Cells Nanomed Biotechnol. 2018; 46:985–993.

[22] Sreenivasulu V, Kumar NS, Suguna M, et al. Biosynthesis of silver nanoparticles using *Mimosa pudica* plant root extract: characterization, antibacterial activity and electrochemical detection of dopamine. Int J Electrochem Sci.. 2016;11:9959–9971.

[23] Francis S, Joseph S, Koshy EP, et al. Microwave assisted green synthesis of silver nanoparticles using leaf extract of *Elephantopus scaber* and its environmental and biological applications. Artif Cells Nanomed Biotechnol. 2018;46:795–804.

[24] Coates J. Interpretation of infrared spectra, a practical approach. *Encyclop Anal Chem*. 2000;12:10818–10837

[25] Srinithya B, Kumar VV, Vadivel V, et al. Synthesis of biofunctionalized AgNPs using medicinally important *Sida cordifolia* leaf extract for enhanced antioxidant and anticancer activities. Mater Lett. 2016;170:101–104.

[26] Kumar V, Singh DK, Mohan S, et al. Photo-induced biosynthesis of silver nanoparticles using aqueous extract of *Erigeron bonariensis* and its catalytic activity against Acridine Orange. J Photochem Photobiol. 2016;155:39–50.

[27] Baláž M, Daneu N, Balážová Ľ, et al. Bio-mechanochemical synthesis of silver nanoparticles with antibacterial activity. Adv. Powder Technol. 2017;28: 3307–3312.

[28] Vijayan R, Joseph S, Mathew B. *Indigofera tinctoria* leaf extract mediated green synthesis of silver and gold nanoparticles and assessment of their anticancer, antimicrobial, antioxidant and catalytic properties. Artif Cells Nanomed Biotechnol.. 2018;46:861–871.

[29] Upadhyay R, Chaurasia JK, Tiwari KN, et al. Antioxidant property of aerial parts and root of *Phyllanthus fraternus* Webster, an important medicinal plant. Sci World J. 2014;[cited 2018 Oct 31]2014:1. [7 p.]

[30] Watanabe A, Kajita M, Kim J, et al. In vitro free radical scavenging activity of platinum nanoparticles. Nanotechnology. 2009;[cited 2018 Oct 3120:455105.

[31] Oh KH, Soshnikova V, Markus J, et al. Biosynthesized gold and silver nanoparticles by aqueous fruit extract of *Chaenomeles sinensis* and screening of their biomedical activities. Artif Cells Nanomed Biotechnol. 2018;46:599–606.

[32] Mehrotra V, Mehrotra S, Kirar V, et al. Antioxidant and antimicrobial activities of aqueous extract of *Withania somnifera* against methicillin-resistant *Staphylococcus aureus*. J Microbiol Biotechnol Res. 2017;1:40–45.

[33] Singh K, Panghal M, Kadyan S, et al. Evaluation of antimicrobial activity of synthesized silver nanoparticles using *Phyllanthus amarus* and *Tinospora cordifolia* medicinal plants. J Nanomed Nanotechnol. 2014;5:1.

[34] Shrivastava S, Bera T, Roy A, et al. Characterization of enhanced antibacterial effects of novel silver nanoparticles. Nanotechnology. 2007;18:225103. [cited 2018 Oct 31]

[35] Lee KY, Jang GH, Byun CH, et al. Zebrafish models for functional and toxicological screening of nanoscale drug delivery systems: promoting preclinical applications. Biosci Rep.. 2017;37:BSR20170199. [cited 2018 Oct 31

[36] Prabhu D, Arulvasu C, Babu G, et al. Biologically synthesized green silver nanoparticles from leaf extract of *Vitex negundo* L. induce growth-inhibitory effect on human colon cancer cell line HCT15. Process Biochem. 2013;48:317–324.

[37] Reddy NJ, Vali DN, Rani M, et al. Evaluation of antioxidant, antibacterial and cytotoxic effects of green synthesized silver nanoparticles by *Piper longum* fruit. Mater Sci Eng C. 2014;34:115–122.

[38] Sankar R, Karthik A, Prabu A, et al. *Origanum vulgare* mediated biosynthesis of silver nanoparticles for its antibacterial and anticancer activity. Colloids Surf B Biointerfaces.. 2013;108:80–84.

[39] Xia T, Kovochich M, Brant J, et al. Comparison of the abilities of ambient and manufactured nanoparticles to induce cellular toxicity according to an oxidative stress paradigm. Nano Lett. 2006;6:1794–1807.